Journal of Chemical, Biological and Physical Sciences

An International Peer Review E-3 Journal of Sciences

*Available online at*www.jcbsc.org

Section A: Chemical Sciences

CODEN (USA): JCBPAT Research Article

Spectroscopic, Characterization and Biological Evaluation of Metal Complexes of 4-(Di 1, 3-(2-Hydroxybenzylidene) Guanidino) Benzoic Acid Ligand

[*1] Abdou Saad El-Tabl, [2] Moshira Abd-Elwahed, [3] mohamed Ahmed Wahba and [1] Moustafa Hemid Mohammed

[*1] Department of Chemistry, Faculty of Science, El-Menoufia University, Shebin El-Kom, Egypt.

[2] Department of Pathology, Faculty of Medicine, El-Menoufia University.

[3] Department of Inorganic chemistry, National Research centre, P.O.12311, Dokki, Cairo, Egypt.

Received: 29 July 2015; **Revised:** 1 September 2015; **Accepted:** 14 September 2015

Abstract: The ligand 4-(di 1,3- (2-hydroxybenzylidene) guanidino) benzoic acid reacted with Cr (III), Mn (II), Fe (III), Co (II), Ni (II), Cu (II), Zn (II), Cd (II), Sr (II), Hg (II), Ag (I), Tl (I), ZrO (II) and UO_2 (II) ions forming octahedral or square planar complexes. These complexes have been synthesized and characterized by elemental analyses, IR, UV- Vis spectra, mass spectra (ligand and its cadmium(II) complex), ^{1}H-NMR spectra (ligand and its mercury(II) complex), magnetic moments, conductances, thermal analyses (DTA and TGA) and ESR measurements. The IR data show that, the ligand behaves as dibasic hexadentate, **(2), (4), (5), (6), (12)** and **(13) ,** dibasic tetradentate**, (3), (8), (9)** and **(10)** mono-basic tetradentate, **(7), (11), (14)** and **(15)**. Molar conductances in DMF indicate that, the complexes are non- electrolyte. The ESR spectra of solid Cu (II) complex **(3)** at room temperature show axial type symmetry, indicating a $d_{(x2-y2)}$ ground state with significant covalent bond character in square planar geometry. However, Cu

(II) complex **(2)** shows broad signals in the low and high field regions indicating spin exchange interactions take place between Cu (II) ions through deprotonated hydroxyl group. Complexes of Mn (II) **(5)** , Co(II), **(6)**, Cr (III), **(12)** and Fe (III)**, (13)** show isotropic type, indicating octahedral structure around the metal ion. Cu (II) complex **(2)**, Ni (II) complex **(4)**, UO_2 (II) complex **(7)**, Hg (II) complex **(8)** and Fe (III) complex **(13)** showed inhibitory effect on liver carcinoma (HePG- 2 cell line) in comparing with the standard drug (Sorafenib), Also, Cu (II) complex **(3)** Ni (II) complex **(4)** and Cd (II) complex **(10)** show Antibacterial activity. Hg (II) complex **(8)**, Cd (II) complex **(10)** and Tl (I) complex **(11)** show antifungal activity.

Keywords: Guanidine ligand and its complexes, Magnetism, Spectroscopy, Biological activity.

INTRODUCTION

Guanidines are the imido derivatives of urea which carry three nitrogen functions - one imine and two amine units[1]. The special assembly is the origin of the most significant characteristic of guanidines their extremely high basicity due to the planar arrangement of the central carbon atom and the three nitrogen atoms attached to it[2]. The benzoyl substituted guanidines have shown good bactericidal and fungicidal properties[3] against several microbial strains, while polyhexamethylene biguanide (PHMB) and polyhexamethylene guanidine (PHMG) were broad spectrum antibacterial agents[4]. Guanidinium-based molecules were also extensively used as cardiovascular drugs[5], antihistamines[6], anti-inflammatory agents[7,8], antidiabetic drugs[9], antibacterial and antifungal drugs[10], antiprotozal and other antiparasitic drugs[11] and antiviral drugs[12].

A chitosan derivative, quaternized carboxymethyl chitosan containing guanidine groups (QGCMC), demonstrated a strong antimicrobial activity at acidic, neutral, and basic pH conditions and could significantly lengthen the shelf life of strawberries[13]. Aminoguanidine and related derivatives were effective in inhibiting nitric oxide production in cells expressing inducible nitric oxide synthase (NOS_2)[14,15] and therefore, aminoguanidines exhibit protective effect against nephrotoxicity[16] and ototoxicity[17] induced by chemotherapeutic agents aminoguanidine moieties present potential use as safe antitumour drugs.

Guanidine is effective inhibitor of corrosion of mild steel, acts as cathodic inhibitor, is temperature independent and the addition of Guanidine decreases the activation energy[18]. A large number of organic compounds having guanidine functionality and metal based drugs are potent antibiotic agents. Polycyclic guanidine alkaloids extracted from sponge Monanchora unguifera[19] and a dimeric bromopyrrole alkaloid, nagelamide G isolated from the Okinawan marine sponge Agelassp. Exhibited antibacterial activity against several bacterial strains[20]. Due to guanidine compounds importance, we reported, synthesis, spectroscopic characterization and biological activity of new ligand 4-(di 1, 3- (2-hydroxy-benzylidene) guanidino) benzoic acid and its metal complexes.

EXPERIMENTAL

Materials: All the reagents employed for the preparation of the ligand and its metal complexes were of the best grade available and used without further purification.

Physical measurements: C, H, N and Cl analyses were determined at the Analytical Unit of Cairo University, Egypt. A standard method was used to determine metal ion[21]. All metal complexes were dried under vacuum over P_4O_{10}. The IR spectra were measured as KBr and CeBr pellets using a Perkin-Elmer 683 spectrophotometer (4000-200 cm^{-1}). Electronic spectra (qualitative) were recorded on a Perkin-Elmer 550 spectrophotometer. The conductance of 10^{-3} M solutions of the complexes in DMF were measured at 25°C with a Bibby conductimeter type MCl. ^{1}H-NMR spectra of the ligand and its Hg (II) complex were obtained with Perkin-Elmer R32-90-MHz spectrophotometer using TMS as internal standard. Mass spectra of the ligand and its Cd (II) complex were recorded using JEULJMS-AX-500 mass spectrometer provided with data system. The thermal analyses (DTA and TGA) were carried out in air on a Shimadzu DT-30 thermal analyzer from 27 to 800°C at a heating rate of 10°C per minute. Magnetic susceptibilities were measured at 25°C by the Gouy method using mercuric tetrathiocyanato cobalt (II) as the magnetic susceptibility standard. Diamagnetic corrections were estimated from Pascal's constant[22]. The magnetic moments were calculated from the equation:

$$\mu_{eff} = 2.84\sqrt{\chi_M^{corr}.T}$$

The ESR spectra of solid complexes at room temperature were recorded using a varian E-109 spectrophotometer, DPPH was used as a standard material. The T.L.C of all compounds confirmed their purity.

PREPARATION OF THE LIGAND AND ITS METAL COMPLEXES

Preparation of the ligand, [H_2L], (1): Ligand **(1)** was prepared by refluxing equimolar amounts of urea (0.6 g, 0.01 mol) and 4-aminobenzoic acid (1.37 g, 0.01mol) in ethanol (100 cm^3) for 2 hour with stirring. The resulting product, 4-guanidinobenzoic acid, (1 g, 0.006 mol) was added to (1.363 g, 0.012 mol) of salicyl-aldehyde in ethanol (100 cm^3) for 2 hour with stirring. The yellow product, was obtained after cooling at room temperature, washed several times with ethanol and dried in vaccuo over $P_4O_{10.}$ Analytical data are given in **Table-1.**

Synthesis of metal complexes (2) – (20): To the ligand (5.0 g, 0.015 mol) in ethanol (50 cm^3) was added (3.2 g, 0.015 mol) of Cu (OAc) $2.H_2O$, complex **(2)**, (2.51 g, 0.015 mol) $CuCl_2.2H_2O$, complex **(3)**, (3.65 g, 0.015 mol) of Ni $(OAc)_2$. $4H_2O$, complex **(4)**, (3.60 g, 0.015mol) of Mn $(OAc)_2$. $4H_2O$, complex **(5)**, (3.66 g, 0.015 mol) Co $(OAc)_2$. $4H_2O$, complex **(6)**, (6.66 g, 0.015 mol) of UO_2 $(OAc)_2$. $2H_2O$, complex **(7)**, (4.95 g, 0.015 mol) of Hg $(OAc)_2$. H_2O, complex **(8)**, (3.23 g, 0.015) Zn $(OAc)_2$. $2H_2O$, complex **(9)**, (3.65 g, 0.015 mol) of Cd $(OAc)_2$. H_2O, complex **(10)**, (3.87 g, 0.015) Tl$(OAc)_,$ complex **(11)**, (3.92 g, 0.015 mol) of $CrCl_3.6H_2O$, complex **(12)**, (3.98 g, 0.015 mol) of $FeCl_3.6H_2O$, complex **(13)**, (3.92 g, 0.015 mol) of $SrCl_2.6H_2O$, complex **(14),** (3.68 g, 0.015 mol) of $ZrOCl_2.4H_2O$, complex **(15)**, (2.49 g, 0.015 mol) of $AgNO_3$, complex **(16)**.

The mixture was refluxed with stirring for 2-4 hour range depending onto nature of metal ion. When the precipitate appeared after adding three drops of dimethylamine, it was removed by filteration, washed with ethanol and dried in vaccuo over $P_4O_{10.}$ Analytical data are given in **Table-1.**

BIOLOGICAL STUDIES

Antitumor: The cytotoxic activity of ligand and its metal complexes were measured invitro for the synthesized complexes using the Sulfo Rhodamine-B-stain (SRB) assay using the puplished methods[23].

Cells were plated in 96-multiwell plate (10^4 cells/well) for 24 hrs before treatment with the compounds to allow attachment of cell to the wall of the plate. Different concentrations of the compounds in DMSO under test (0, 1.56, 3.125, 6.5, 12.5 and 25 µg/ml) were added to the cell monolayer triplicate wells were prepared for each individual dose. Monolayer cells were incubated with the compounds for 48 hrs at 37°C using 5% CO_2.

After 48 hrs, cells were fixed, washed and stained with Sulfo-Rhodamine-B-stain. Excess stain was wash with acetic acid and attached stain was recovered with tris EDTA buffer (10 mM tris HCl + 1 mM disodium EDTA, PH 7.5-8). Color intensity was measured in an ELISA reader. The relation between surviving fraction and drug concentration is plotted to get the survival curve of each tumor cell line after the specified compound.

Antifungal activity: Fungicidal activity of tested complexes was assessed against Aspergillus niger by disc diffusion method

Testing method: Base layer was obtained by pouring about 10-15 ml of base layer medium into each sterilized petri dishes and were allowed to attain at room temperature. Overnight grown subcultures of fungi were mixed with layer medium and immediately poured into petri dishes containing the base layer and then allowed to attain at room temperature. Antifungal discs having diameter of 6 mm, soaked in test solution, were dispensed on to the surface of inoculated agar plate.

Each disc must be pressed down to ensure its complete contact with the agar surface. These plates were subsequently incubated at 37° C for 36 hours. The zone of inhibition, if any, was measured in mm for the particular complex. Clotrinazole was used as positive control and solvent control (12 mm) was also used to know the activity of the solvent.

Antibacterial activity: Antibacterial activity of tested complexes was assessed against gm (+)ve bacteria Streptococcus and Enterococcus and gm (-)ve bacteria Klebsiella pneumoniae and Salmonella by disc diffusion method.

Testing method: The method of testing for antibacterial activity is the same as that adopted for assessing antifungal. Linezolid was used as positive control and solvent control (12 mm) was also used to know the activity of the solvent.

RESULTS AND DISCUSSION

The analytical and physical data (**Table-1**), spectral data (**Tables 2** and **3**) revealed that, the complexes are formed in (1:1) or (1:2) (L: M) stiochiometric ratio. All the complexes are stable at room temperature, insoluble in common solvents, viz: MeOH, EtOH, $CHCl_3$, CCl_4 and $(CH_3)_2CO$ but soluble in DMSO [21, 22] the analytical and spectral data are compatible with the proposed structure, **Figure (1)**. 4-(di 1,3 (2-hydroxybenzylidene)guanidino)benzoic acid **(1),** was synthesized by refluxing of 4-guanidinobenzoic acid with salicylaldehyde in ethanol (100 cm^3) for 3 hour with stirring (1:2), molar ratios as shown in **Figure (2)**.

Table-1: Analytical and Physical Data of the Ligand [H_2L] and its Metal Complexes.

No.	Ligands/Complexes	Color	FW	M.P (^{O}C)	Yield (%)	Anal. /Found (Calc.) (%)					Molar conductance Λm (Ω^{-1} cm^2 mol^{-1})
						C	H	N	M	Cl	
(1)	[H_2L] $C_{22}H_{19}N_3O_5$	Dark yellow	405	-	90	65.9(65.18)	5.01(4.72)	9.95(10.37)		-	-
(2)	[(L) Cu_2 $(OAc)_2$ $(H_2O)_4$].$2H_2O$ $C_{26}H_{33}N_3O_{14}Cu_2$	Green	737	>300	75	42.28(41.8)	4.5(4.48)	5.69(5.46)	17.21(17.49)	-	12.3
(3)	[(L) Cu].H_2O $C_{22}H_{17}N_3O_5Cu$	Green	466.93	>300	69	56.47(56.59)	4.25(3.67)	9.7(9.00)	14.7(13.61)	-	11.6
(4)	[(L) Ni_2 $(OAc)_2$ $(H_2O)_4$]. $2H_2O$ $C_{26}H_{33}N_3O_{14}Ni_2$	Greenish yellow	728.94	>300	61	42.84(42.08)	4.56(5.1)	5.76(6.16)	16.1(16.59)	-	13.8
(5)	[(L) Mn_2 $(OAc)_2$ $(H_2O)_4$]. $2H_2O$ $C_{26}H_{33}N_3O_{14}Mn_2$	Dark brown	721.43	>300	59	43.29(43.66)	4.61(4.75)	5.82(5.15)	15.23(15.6)	-	14.1
(6)	[(L) Co_2 $(OAc)_2$ $(H_2O)_4$]. $2H_2O$ $C_{26}H_{33}N_3O_{14}Co_2$	Yellow	729.42	>300	55	42.81(42.2)	4.56(5.3)	5.76(5.9)	16.16(16.88)	-	15.0
(7)	[(HL) (UO_2)(OAc). (H_2O)].$4H_2O$ $C_{24}H_{29}N_3O_{13}U$	Yellow	805.5	>300	54	35.5(35.78)	3.44(3.63)	5.5(5.22)	29.95(29.55)	-	11.8
(8)	[(L) Hg_2 $(H_2O)_2$].4 H_2O $C_{22}H_{27}N_3O_{10}Hg_2$	Pale green	694	280	61	38.07(38.16)	3.92(3.57)	6.05(5.71)	28.9(28.25)	-	14.2
(9)	[(L) Zn_2 $(H_2O)_2$].4 H_2O $C_{22}H_{27}N_3O_{10}Zn_2$	Greenish yellow	558.85	>300	59	47.28(47.97)	4.87(4.8)	7.52(6.99)	11.7(10.88)	-	12.7
(10)	[(L) Cd_2 $(H_2O)_2$].4 H_2O $C_{22}H_{27}N_3O_{10}Cd_2$	Dark Yellow	605.87	>300	55	43.61(44.49)	4.49(4.51)	6.94(6.59)	18.55(18.35)	-	13.2
(11)	[(HL) Tl_2(OAc) $(H_2O)_2$] $C_{24}H_{23}N_3O_8Tl_2$	Pale Yellow	890.22	>300	51	31.61(32.38)	2.89(2.6)	5.1(4.72)	45.55(45.92)	-	18.1
(12)	[(L) $Cr_2(Cl_4)$ $(H_2O)_2$].$4H_2O$ $C_{22}H_{27}Cl_4$ $N_3O_{10}Cr_2$	Pale Green	739.27	>300	65	35.74(35.09)	3.68(4.35)	5.68(6.1)	14.07(14.5)	19.18(19.83)	18.4
(13)	[(L) $Fe_2(Cl_4)$ $(H_2O)_2$].$4H_2O$ $C_{22}H_{27}Cl_4$ $N_3O_{10}Fe_2$	Brown	746.97	>300	62	35.37(35.81)	3.64(4.13)	5.63(6.07)	14.95(14.26)	18.99(18.75)	20.1
(14)	[(HL) Sr(Cl) (H_2O)].$2H_2O$ $C_{22}H_{22}Cl$ N_3O_7Sr	Beige	563.5	>300	55	47.2(46.89)	4.35(3.94)	7.85(7.46)	16.2(15.55)	6.9(6.29)	19.2
(15)	[(HL) ZrO(Cl) (H_2O)].$4H_2O$ $C_{22}H_{26}Cl$ $N_3O_{10}Zr$	Yellow	619.13	>300	65	43.1(42.68)	4.65(4.23)	6.2(6.79)	15.1(14.73)	5.38(5.73)	20.1
(16)	[$(H_2L)Ag(NO_3)$]H_2O	Yellow	575.28	>300	75	46.2 (45.93)	3.45(3.33)	9.36 (9.74)	19.2(18.75)	-	19.7

Table-2: IR frequencies of the bands (cm^{-1}) of ligand [H_2L] and its Metal Complexes and their assignments.

No.	ν(H_2O/OH)	ν (H-bond.)	ν(C=O)$_{acetyle}$	ν(C=N)$_{imine}$	ν(Ar)	υ (OAc) /NO_3/SO_4	υ(M-O)	Y(M-N)	υ(M-Cl)
(1)	3460,3429;3600-3150	3520-3100,2950-2580	1682	1660,1606	1595,7571491,854	-	-	-	-
(2)	3427,3175;3575-3200 3150-2850	3530-3150,2780-2530	1680	1650,1600	1595,7621490,865	1539,1397	709	483	-
(3)	3421;3530-3200	3510-3100,3050-2850	1680	1620, 1596	1561,7581537,865	-	709	485	-
(4)	3420 ,3630-3280 3250-3080	3540-3110,3100-2620	1681	1620,1598	1547,758,1470,867	1443,1375	683	592	-
(5)	3422,3560-3220 3200-3050	3500-3080,3080-2650	1680	1620,1597	1542,7561468,862	1445,1395	704	520	-
(6)	3430, 3550-3270 3230-2970	3520-3110,3090-2680	1678	1620,1597	1550,766,1468,865	1468,1400	711	525	
(7)	3433,3379, 3595-3250 3220-3070	3525-3150,3125-2620	1680	1620,1603	1545,6751465,788	1525,1409	634	474	-
(8)	3428,3575-3220 3200-3060	3540-3110,3030-2620	1680	1620,1589	1555,753,1477,861	---	668	521	-
(9)	3408,3570-3230 3210-3080	3545-3100,3050-2720	1681	1619,1600	1565,758,1463,866	----	683	496	-
(10)	3431,3580-3260 3220-3020	3510-3080,3030-2620	1680	1617,1597	1575,750,1467,862	---	681	495	-
(11)	3433,3360 3550-3200	3530-3100.3080-2620	1682	1620,1597	1577,745,1530,857	1503,1381	674,698	524	409
(12)	3421,3630-3260 3240-3110	3585-3145,3060-2695	1679	1618,1603	1564,7611470,857	-	707	532	445
(13)	3423 ,3610-3100 3080-2800	3570-3150,3050-2720	1678	1611,1599	1539,762 1469,862	-	703, 657	521,483	422
(14)	3422, 3390,3620-3220 3180-2960	3540-3180,3080-2750	1680	1610,1600	1521,749 1499,858	-	603	524	421
(15)	3428,3390,3615-3200 3150-2750	3590-3110,3015-2790	1681	1615,1602	1545,757 1475,861	-	785	546	443
(16)	3455,3430,3650-3010	3620-3150,3050-2540	1684	1621,1606	1582,784,1498,859	1376,1171, 33,785	-	532	

Table-3: The electronic absorption spectral bands (nm) and magnetic moment (B.M) for the ligand [H_2L] and its complexes.

No.	λ_{max}^{*} (ε)	μ_{eff} in BM
(1)	265nm ϵ = 6.4×10^{-3} $mol^{-1}cm^{-1}$) 325nm ϵ = 7.8×10^{-3} $mol^{-1}cm^{-1}$) 395nm(ϵ = 9.5×10^{-3} $mol^{-1}cm^{-1}$)	-
(2)	262,305,380,450,589,641,719	1.42
(3)	255,315,391,455,515,565	2.12
(4)	260,320,390,458,521,651,727	2.96
(5)	255,320,390,460,532,595,654,	3.13
(6)	255,302,392,585,654,	2.57
(7)	262,320,395	Diamagnetic
(8)	255,300,390	Diamagnetic
(9)	257,320,392	Diamagnetic
(10)	258,315,391	Diamagnetic
(11)	260,310,380,425	2.1
(12)	250,315,390,465,525,546,658	2.98
(13)	260,305,385,460, 570,649	3.08
(14)	257,311,385	diamagnetic
(15)	258,315,391,	diamagnetic
(16)	255,310,390,	diamagnetic

* in nm

Table-4: ESR data for the metal complexes.

No.	$g_{\|}$	$g_{\perp}$	g_{iso} [a]	$A_{\|}$	$A_{\perp}$	A_{iso} [b]	G [c]	ΔE_{xy}	ΔE_{xz}	$K_{\perp}^2$	$K_{\|}^2$	K	$g_{\|}/A_{\|}$	α^2	β^2	β_1^2	2β	a_d^2 (%)
(3)	2.26	2.06	2.13	190	15	73.3	4.3	17699	21978	0.75	0.76	0.85	113	0.95	0.79	0.71	-212	90.5%
(5)			2.006															
(6)			2.006															
(12)			2.11															
(13)			2.13															

a) $3g_{iso} = g_{\|} + 2g_{\perp}$ b) $3A_{iso} = A_{\|} + 2A_{\perp}$ c) $G = g_{\|} - 2 / g_{\perp} - 2$

Table-5: Thermal data for the metal complexes.

No.	**Temp. (^{o}C)**	**DTA (Peak)**	**TGA (wt. loss %)**		**Assignment**
			Calc.	**Found**	
(2)	40	Endo	-	-	broken of hydrogen bond
	75	Endo	4.88	5.4	Loss of two hydrated water
	137	Endo	10.27	10.77	Loss of 4 coordinated water
	291	Endo	18.75	19.11	Loss of two coordinated acetate group
	416	Endo	-	-	Melting point
	456,500	Exo	16.73	17.2	Decomposition and formation of 2CuO
(4)	59	Endo	4.9	4.46	Loss of two hydrated water
	182	Endo	10.4	10.7	Loss of 4 coordinated water
	331	Endo	19.03	19.6	Loss of two acetate group
	386	Endo	-	-	Melting point
	450, 490, 540, 575	Exo	29.48	28.9	Decomposition and formation of 2NiO
(9)	51	Endo	12.88	13.33	Loss of 4 hydration water
	173	Endo	7.39	7.5	Loss of 2 coordinated water
	444	Endo	-	-	Melting point
	450.500,590	Exo	-	-	Decomposition and formation of ZnO
(13)	59	Endo	11.2	11.9	Loss of 4 hydrated water
	135	Endo	18.5	19.1	Loss of 3 coordinated cholrine group
	351	Endo	-	-	Melting point
	450, 549, 578, 621, 674	Exo	34.15	35.2	Decomposition and formation of Fe_2O_3

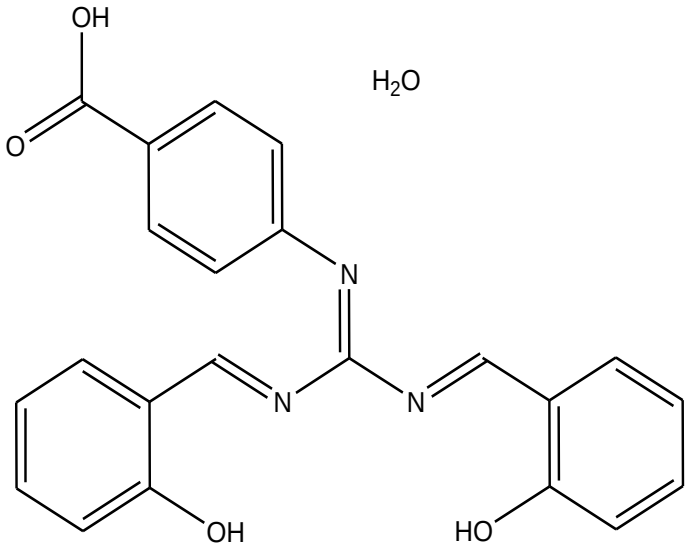

Ligand (1)

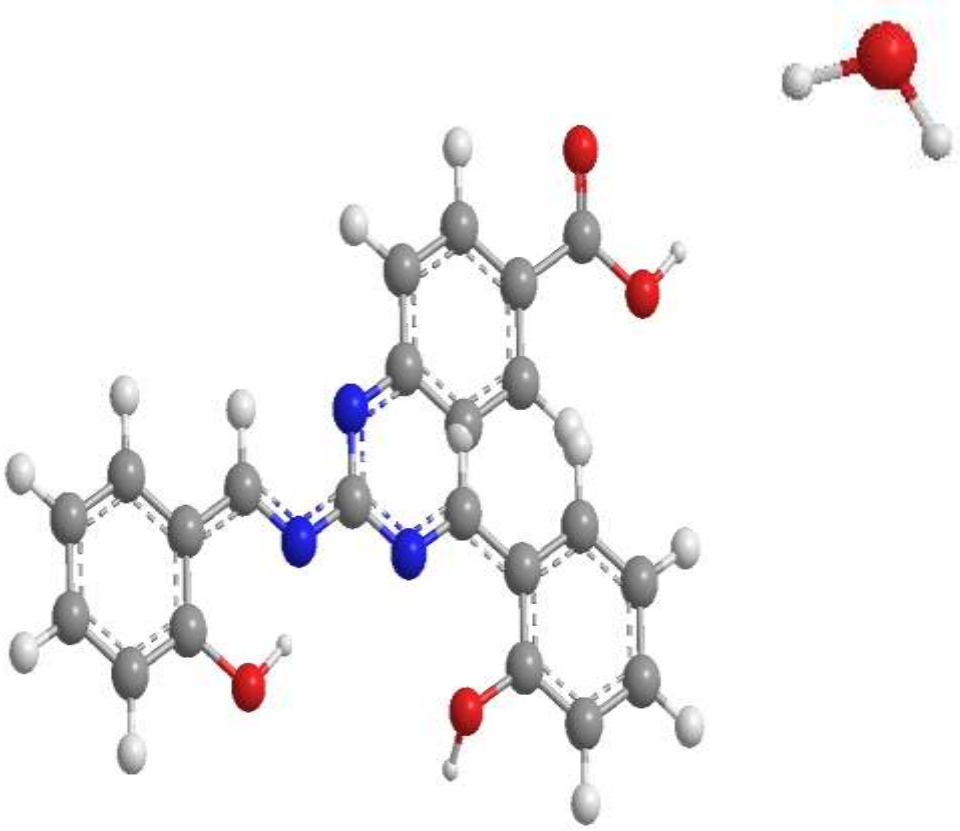

Ligand (**1**)

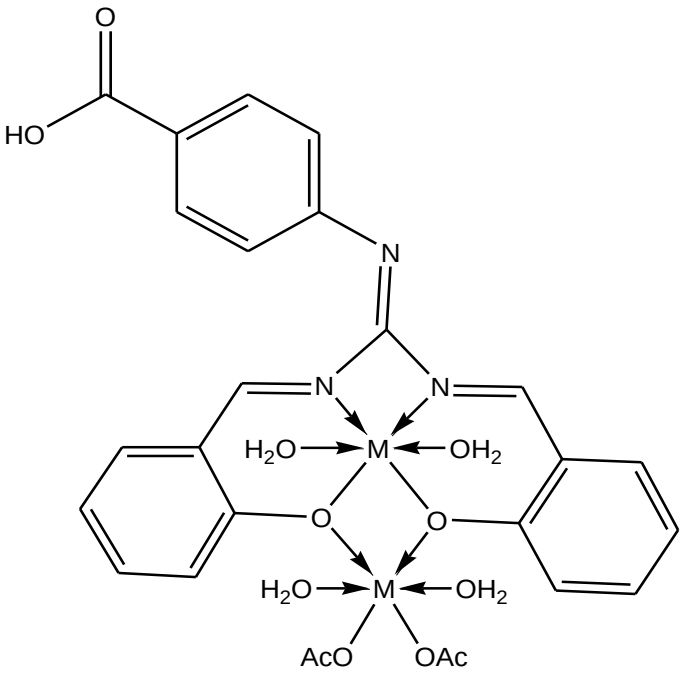

nH_2O

M = **Cu** (II) n=**2** Complex (**2**)

M = **Ni** (II) n=**2** Complex (**4**)

M = **Mn** (II) n=**2** Complex (**5**)

M = **Co** (II) n=**2** Complex (**6**)

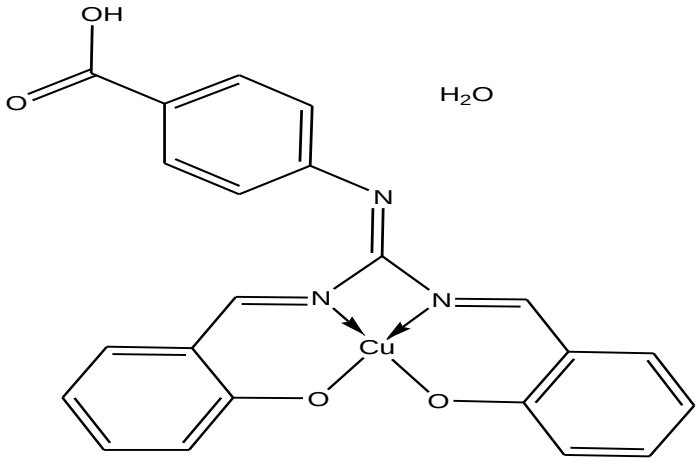

Complex **(3)**

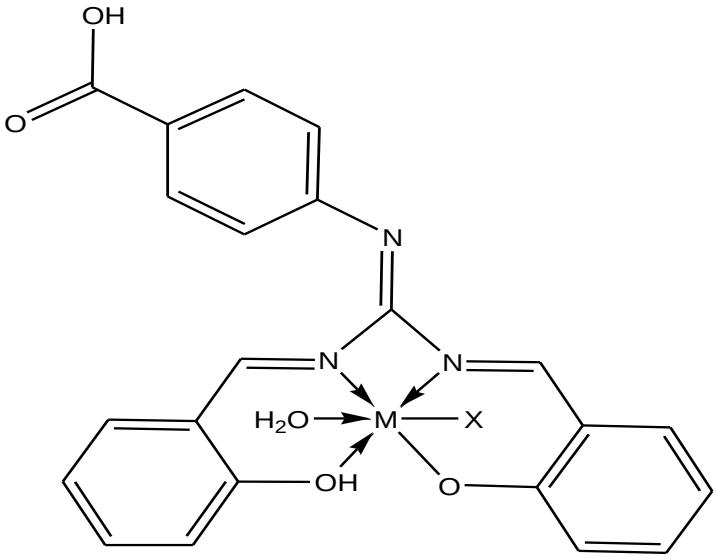

nH_2O

M = **UO_2** (II) n=**4** X= OAc Complex (**7**)

M = **Sr** (II) n=**2** X= Cl Complex (**14**)

M = **ZrO** (II) n=**4** X= Cl Complex (**15**)

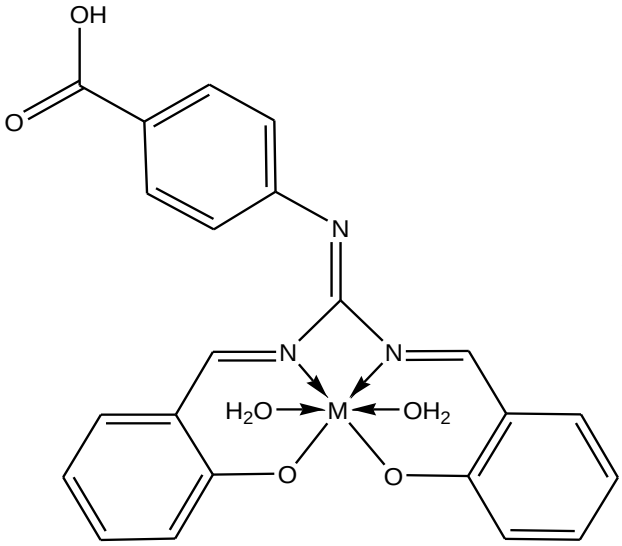

nH_2O

M = **Hg** (II) n=**4** Complex **(8)**

M = **Zn** (II) n=**4** Complex (**9**)

M = **Cd** (II) n=**4** Complex (**10**)

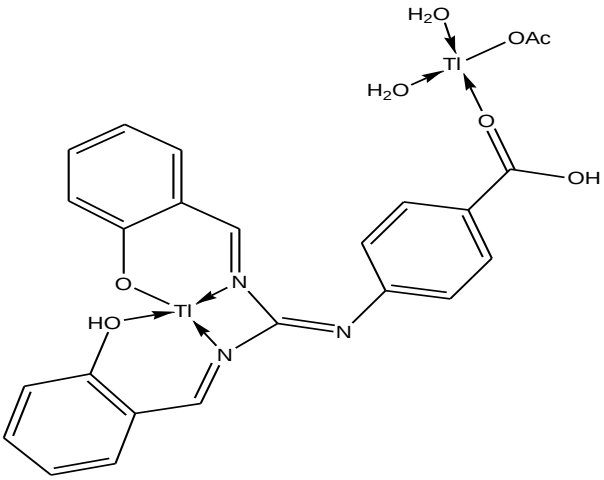

Complex **(11)**

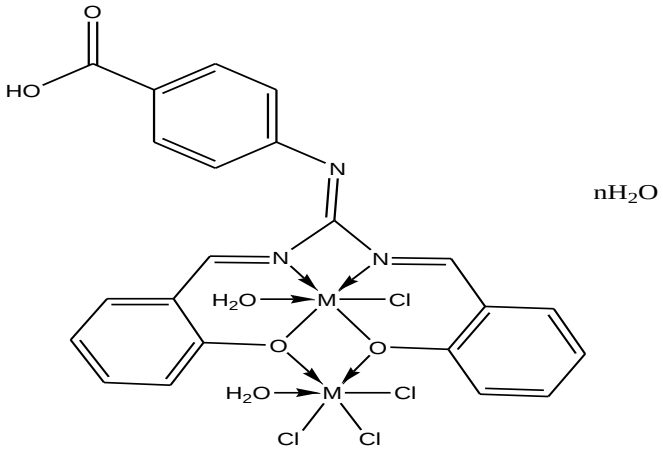

M = **Cr** (III) n=**4** Complex (**12**)
M = **Fe** (III) n=**4** Complex (**13)**

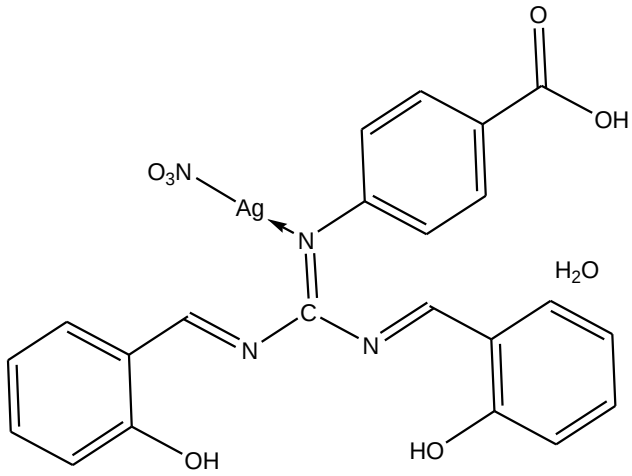

Complex (**16**)

Figure 1: Suggested structures of the ligand and its metal complexes.

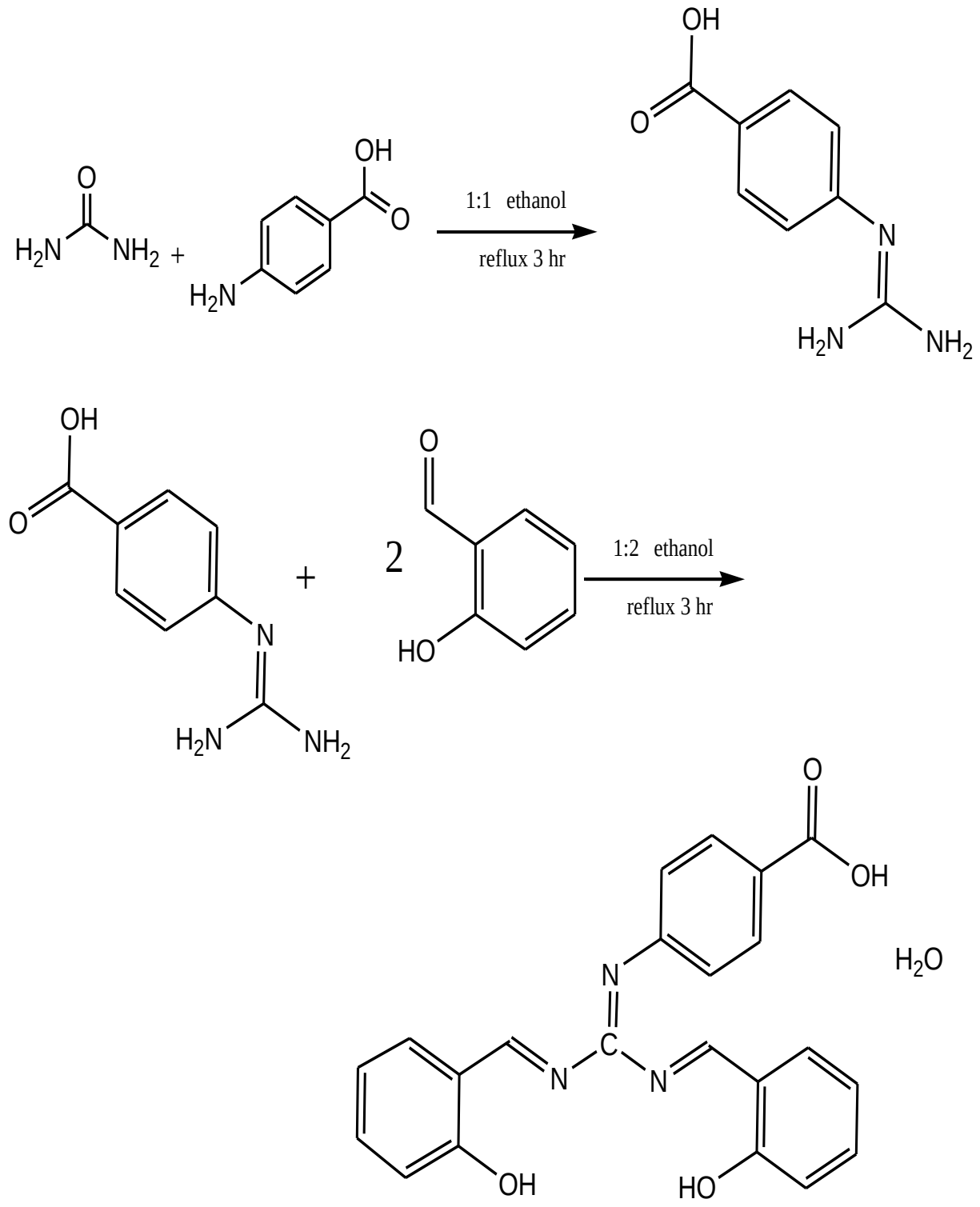

Scheme (1)

Figure 2: Illustrates that, the composition of the complexes formed depending on the metal salts, solvent and the molar ratios.

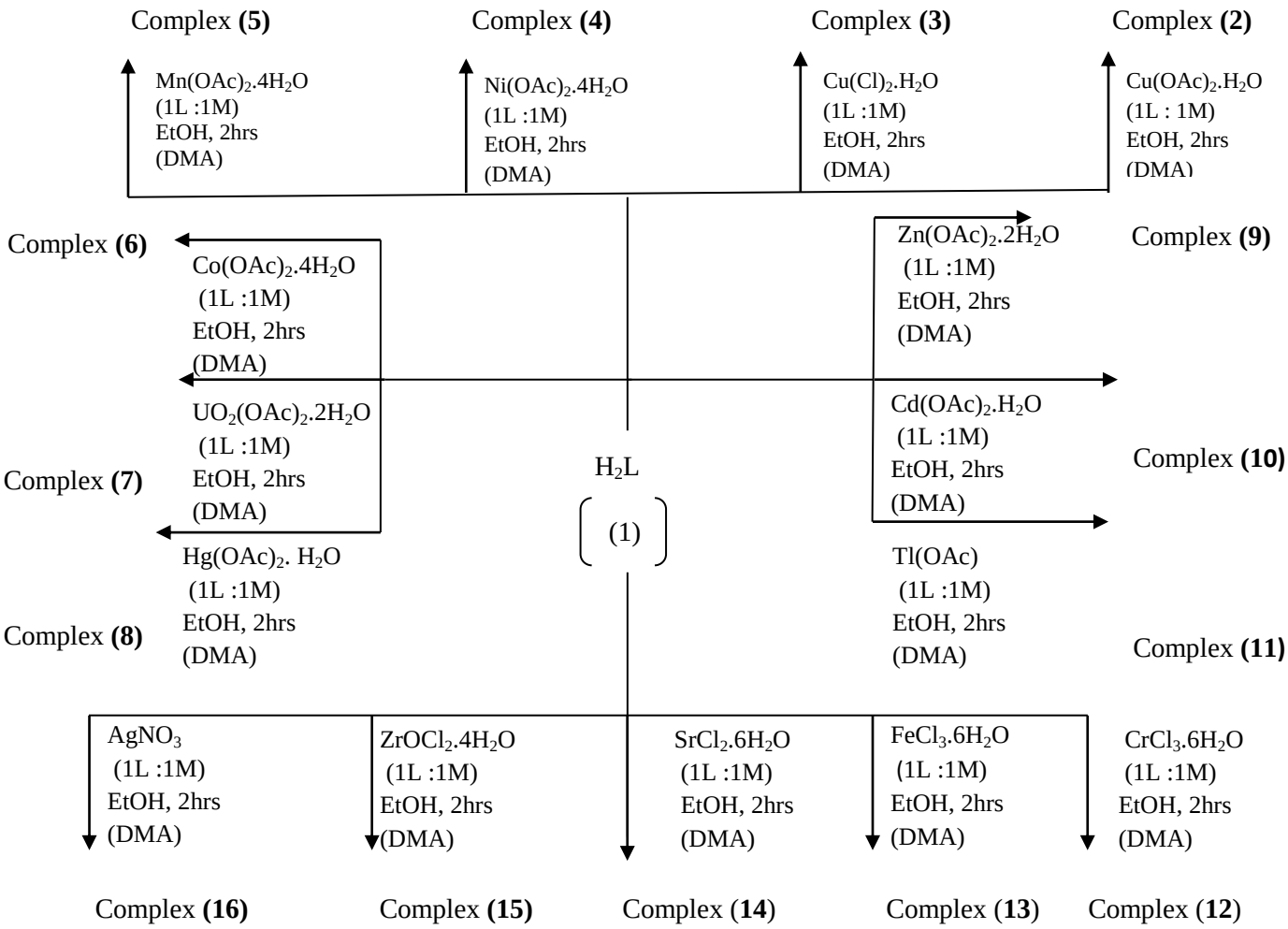

DMA= dimethyl amine

Scheme-1

Mass Spectra of the Ligand, (1) And Its Cd (II) Complex (10): The mass spectra of the ligand **(1)** and its Cd (II) complex **(10)** confirmed their proposed formulations. The mass spectrum of the ligand, **(1)** supported, the suggested structure, (**Figure 1**) and revealing a molecular ion peak (m/z) at 405 a.m.u., constitute of the molecular weight of the ligand. Morever, the fragmentation pattern splits a parent ion peak at m/z = 207 a.m.u. corresponding to $C_{15}H_{11}N_3O_2$ while the fragments at m/z =121, 236, 266 and 344 a.m.u. are due to $C_{14}H_{11}N_2$, $C_{14}H_{10}N_3O$, $C_{15}H_{12}N_3O_2$ and $C_{21}H_{16}N_3O_2$, moieties respectively. The mass spectrum of Cd (II) complex **(10)** supported, the suggested structure, (**Figure 1**) and revealing a molecular ion peak (m/z) at 606 a.m.u, compatible with the molecular weight of the complex (605.8). Additionally, the fragmentation pattern splits a parent ion peak at(m/z) = 135 a.m.u. corresponding to $C_7H_5NO_2$ while the fragments at (m/z) = 221, 229, 268, 297, 371, 379, 399 and 535 a.m.u. are due to $C_2H_7N_2O_3Cd$, $C_4H_6NO_3Cd$, $C_7H_9NO_3Cd$, $C_8H_{11}N_2O_3Cd$, $C_{15}H_{17}N_2O_2Cd$, $C_{11}H_{12}N_3O_5Cd$, $C_{15}H_{14}N_2O_4Cd$ and $C_{22}H_{19}N_3O_6Cd$, moieties respectively. The fragments of **(1)** and Cd (II) complex **(10)** are represented in **Table-6**.

^{1} H – NMR spectra: The ^{1}H – NMR spectra of (**1**) and its Hg (II) complex **(8)** in deuterated DMSO shown signals consistent with the proposed structure. The ligand shows singlet peaks at 10.7 and 10.25 p.p.m is due to proton of OH group[24,25]. The singlet signal observed at 8.8 p.p.m, are due to the protons of HC=N group[26]. However, the peaks observed as multiple ones in the 6.6 – 7.9 p.p.m range may be assigned to aromatic protons[27]. The spectrum of mercury(II) complex **(8)** shows, the proton of carboxylic OH group at 12 and the singlet signal characteristic to the phenolic hydroxyl group (OH) disappeared, indicating that, deprotonated hydroxyl group participate in the coordination[28]. The aromatic protons and the protons of HC=N group appear in the 6.6 -7. 8 p.p.m range[29]. A new signal was observed at 2.4 p.p.m which may be assigned to the protons of the coordinated water[26,30].

Conductivity: The molar conductance values of the complexes in DMF (10^{-3} M) lie in the 21.2 – 11.3 Ω $mol^{-1}cm^2$ range (**Table-1**), indicating that, all the complexes are not electrolytes[29,31]. This confirms that, the anion is coordinated to the metal ion.

IR SPECTRA

The modes of bonding between the ligand and the metal ion can be revealed by comparing the IR spectra of the solid complexes with that of the ligand. The IR spectral data of the ligand and its metal complexes are presented in **Table-2)**. The IR spectrum of **(1)** shows broad medium bands in the 3520-3100 and 2950-2580 cm^{-1} ranges, attributed to intra- and intermolecular hydrogen bonds between aromatic OH with imine or carbonyl groups[32, 33]. Thus, the higher frequency band is associated with a weaker hydrogen bond and the lower frequency band with a stronger hydrogen bond. Also, the spectrum shows bands at 3460 and 3429 cm^{-1}, assigned to the stretching vibrations of the phenolic and aliphatic carboxylic hydroxyl ν (OH) associated with hydrogen bondings[26, 34, 35].

The relatively strong bands located at 1682, 1660, 1606, 1595 and 1491 cm^{-1} are assigned to the ν(C=O), (C=N) imine and $\nu(C=C)_{Ar}$ respectively[23]. In all complexes, the band due to azomethine $\nu(C=N)_{imine}$ was shifted with decreasing its intensity (10-50 cm^{-1}) indicating its coordination to the central metal ion[26]. The ν(OH) groups appear in the 3433-3374 and 3560 - 3360 cm^{-1} ranges[36,37] but ν(OH) of the phenolic carboxylic hydroxyl disappear in complexes **(3-6), (8), (9), (10), (12)** and **(13)** .The $\nu(C=C)_{Ar}$ appears in the 1595- 1465 and 867- 675 cm^{-1} ranges[38,39]. All complexes show broad bands in the 3630 – 3100 and 3250 – 2750 cm^{-1} ranges, assigned to the presence of hydrated or coordinated water molecules[38] except complexes **(3)** and **(11)**.

However, the bands appear in the 3590 –3080 and 3125 – 2530 cm^{-1} ranges, are due to intra- and intermolecular hydrogen bondings[40-42]. New bands in the 785 – 603 and 592 – 474 cm^{-1} ranges were taken as indication of coordination between the metal ions with oxygen and nitrogen atoms[37,38]. Extensive IR spectral studies reported on metal acetate complexes[43] indicate that, the acetate ligand coordinates[44] as a monodentate manner and the coordination ν(C=O) appear at higher energy than ν_a (CO_2) and ν(C-O) observed lower than ν_s (CO_2). As a result, the separation between ν (CO) bands is much larger in monodentate complexes. In complexes **(4-7)** and **(11),** the band is due to ν_a (CO_2) appeared in the 1539 – 1443 cm^{-1} and the ν_s (CO_2) observed in the 1409 – 1375 cm^{-1} ranges. The difference between these two bands is in the 130 – 68 cm^{-1} range, suggesting that, the acetate group coordinates in unidentate manner with the metal ions[25]. A new band observed in the 445 – 409 cm^{-1}, may be assigned to ν (M-Cl) in the chloro complexes **(11) – (15)**[45].

Complex **(16)** shows bands at 1376, 1171, 833 and 785, assigned to coordinated nitrate group[32,36]. The complex **(16)** has a monomeric linear planar in which the guanidine coordinates as a pseudomonodentate ligand interacting with silver ion via N_{imine} and nitrate moieties[46]. The appearance of ν (OH) group of ligand at 1284 cm^{-1}. All complexes show ν (OH) band in the 1299 – 1280 cm^{-1}, at higher wave number comparing to the ligand, indicating non- coordinated of this group to the metal ion. Complex **(7)** shows band at 897 cm^{-1} is due to O=U=O[47].

Magnetic moments: The room temperature magnetic moments of the complexes **(2) – (16)** are shown in **Table-3**. Copper(II) complexes **(2)** and **(3)** show values 1.42 and 2.12 B.M., corresponding to one unpaired electron in an octahedral or square planar structure[30,46], as, The complex **(2)** shows lower value, indicating that, spin – exchange interactions takeplace between the copper(II) ions through cobridging[30,47]. Nickel (II) complex **(4)** gives 2.96 B.M., confirmed t_2g^6 eg^2 electronic configuration with two unpaired electrons in an octahedral Ni (II) complex[30,48]. Manganese (II) complex **(5)** and cobalt (II) complex **(6)** show values 3.13 and 2.57 B.M., indicating high spin octahedral structure[30,46], the lower values is due to spin exchange interactions between the metal ions through cobridge. Thallium (I) complex **(11)** gives 2.1 B.M., indicating an octahedral structure.

Chromium (III) complex **(12)** and Iron(III) complex **(13)** show values 2.98 and 3.08 B.M., indicating high spin octahedral structure,[30,49] the lower values of magnetic moments are due to spin exchange interactions takeplace between metal ions. Uranyl (II) complex **(7)**, mercury (II) complex **(8)**, zinc (II) complex **(9),** cadmium (II) complex **(10)**, strontium (II) complex **(14)** zirconyl (II) complex **(15)** and silver (I) complex **(16)** show diamagnetic values.

Electronic spectra: The electronic spectral data for the ligand **(1)** and its metal complexes in DMF solution are summarized in **Table-3**. Ligand **(1)** in DMF solution shows three bands at 395 nm ($\epsilon = 9.5\times10^{-3}$ $mol^{-1}cm^{-1}$), 325 nm ($\epsilon = 7.8\times10^{-3}$ $mol^{-1}cm^{-1}$) and 265 nm ($\epsilon = 6.4\times10^{-3}$ $mol^{-1}cm^{-1}$), which may be assigned to the n→π* and π→π* transitions respectively [50-52]. Copper (II) complexes **(2)** and **(3)** show bands in the 262 – 255, 315 – 305 and 391 – 380 nm ranges, these bands are due to intraligand transitions, however, the complex **(2)** show bands which are appeared at 452, 589 and 641 nm which are assigned to O→Cu charge transfer, $^2B_1 \rightarrow {}^2E$ and $^2B_1 \rightarrow {}^2B_2$ transitions, indicating a distorted tetragonal octahedral structure[24,53,54].

However, complex **(3),** shows bands at 455, 515 and 565 nm which are corresponding to $^2B_{1g} \rightarrow {}^2B_{2g}$, $^2B_{1g} \rightarrow {}^2E_g$ and $^2B_{1g} \rightarrow {}^2A_{1g}$ respectively, suggesting a square planar geometry[55,56]. Nickel (II) complex **(4)** shows bands 260, 320, 390, 458, 651 and 727 nm respectively, the first three bands are within the ligand and the other three bands are attributable to $^3A_{2g}(F) \rightarrow {}^3T_{1g}(P)(\nu_3)$, $^3A_{2g}(F) \rightarrow {}^3T_{1g}(F)(\nu_2)$ and $^3A_{2g}(F) \rightarrow {}^3T_{2g}(F)(\nu_1)$ transitions respectively, indicating an octahedral Ni(II) complex[24,57]. The ν_2/ν_1 ratio for the complex is 1.2, which is less than the usual range of 1.5 – 1.75, indicating a distorted octahedral Ni (II) complex[24,58]. Cobalt (II) complex **(6)** shows bands at 255, 302, 392, 585 and 654 nm, the first three bands are within the ligand and the other bands are assigned to $^4T_{1g}(F) \rightarrow {}^4A_{2g}$ and $^4T_{1g}(F) \rightarrow {}^4T_{2g}(F)$ transitions respectively, corresponding to high spin Co (II) octahedral complexes[59] . Manganese(II) complex **(5)** shows bands at 255, 320, 390, 460, 595 and 654 nm, respectively, the first three bands are within the ligand, however, the other bands are corresponding to $^6A_{1g} \rightarrow {}^4E_g$, $^6A_{1g} \rightarrow {}^4T_{2g}$ and $^6A_{1g} \rightarrow {}^4T_{1g}$ transitions which are compatible to an octahedral geometry around the Mn (II) ion[60]. Tl (I) Complex **(11)** gave bands at 260, 310 and 380 nm, respectively.

These bands are due to intraligand transitions since these bands appear almost in the spectrum of the ligand, additional weak band appears at 425 nm, which may be assigned to the $^1S_0 \rightarrow {}^3P_1$ transition of Tl (I) complex[61]. Iron (III) complex **(13)** shows bands at 260, 305, 385, 460 and 649 nm respectively, the first three bands are within the ligand while the other bands are due to charge transfer and $^6A_1 \rightarrow {}^4T_1$ transitions, suggesting distorted octahedral geometry around the iron (III) ion[61, 62].

While chromium (III) complex **(12)** shows bands at 250, 315, 390, 465, 525 and 658 nm respectively. The first three bands are assigned to $^4A_{2g} \rightarrow {}^4T_{1g}$ (F), $^4A_{2g} \rightarrow {}^4T_{2g}$ and $^4A_{2g} \rightarrow {}^2T_{2g}$ transitions respectively, indicating octahedral structure around the Cr (III) ion[63,64]. Zinc(II) complex **(9)**, uranyl (II) complex **(7)**, mercury (II) complex **(8)**, strontium (II) complex **(14)** and silver (I) complex **(16)** show three bands in the 262 – 255, 320 – 300 and 395 – 385 nm ranges, which are assigned to intraligand transitions.

Electron Spin Resonance (ESR): The ESR spectral data for complexes **(2)**, **(3)**, **(5)**, **(6)**, **(12)** and **(13)** are presented in **Table-4**. The spectra of copper (II) complexes **(2)** and **(3)** are characteristic of species, d^9, configuration and having axial type of a $d_{(x2-y2)}$ ground state which is the most common for copper (II) complexes[65,66]. The complex (**2**) shows broad signals in the low and high field regions indicating spin – spin interactions takeplace between Cu (II) ions through deprotonated hydroxyl group.

The complex (**3**) shows $g_{\|} > g_{\perp} > 2.0023$, indicating square planar geometry around copper (II) ion[67,68]. Complex **(3)** shows G- value 4.3 indicating absence of spin – spin interactions in this complex. However, this phenomenon is further confirmed by magnetic moments (2.1 B.M.). Also, the $g_{\|}/A_{\|}$ values considered as diagnostic of stereochemistry[68], in the range reported for square planar complexes are 105 to 135 cm^{-1} and for tetragonal distorted complexes 150 to 250 cm^{-1}. The $g_{\|}/A_{\|}$ values lie just within the range expected for the complexes (**Table-4**).

The g- value of the copper (II) complexes with a $^2B_{1g}$ ground state ($g_{\|} > g_{\perp}$) may be expressed[69] by

$$g_{\|} = 2.002 - (8K^2_{\|}\lambda^\circ/\Delta E_{xy}) \quad \ldots (1)$$

$$g_{\perp} = 2.002 - (2\,K^2_{\perp}\lambda^\circ/\Delta E_{xz}) \quad \ldots (2)$$

Where $k_{\|}$ and $k_{\perp}$ are the parallel and perpendicular components respectively of the orbital reduction factor (K), λ° is the spin – orbit coupling constant for the free copper, ΔE_{xy} and ΔE_{xz} are the electron transition energies of $^2B_{1g} \rightarrow {}^2B_{2g}$ and $^2B_{1g} \rightarrow {}^2E_g$.

From the above relations, the orbital reduction factors ($K_{\|}$, $K_{\perp}$, K), which are a measure of covalency[70,71] can be calculated. For an ionic environment K=1 and for a covalent environment K<1.The lower the value of k, the greater is the covalency

$$K^2_{\perp} = (g_{\perp} - 2.002)\,\Delta E_{xz}/2\lambda_o \quad \ldots (3)$$

$$K^2_{\|} = (g_{\|} - 2.002)\,\Delta E_{xy}/8\lambda_o \quad \ldots (4)$$

$$K^2 = (K^2_{\|} + 2K^2_{\perp})/3 \quad \ldots (5)$$

K (**Table-4**), for the copper (II) complex **(3)** indicating covalent bond character[46,72]. Kivelson and Neiman[73] noted that, for ionic environment $g_{\|} \geq 2.3$ and for a covalent environment $g_{\|} < 2.3$. Theoretical work by Smith[74] seems to confirm this view. The g- values reported here (**Table-4**) show considerable covalent bond character[46]. Also, the in-plane σ-covalency parameter, α^2 (Cu) was calculated by

$$\alpha^2 (Cu) = (A_{\|}/0.036) + (g_{\|}-2.002) +3/7(g_{\perp} -2.002) +0.04. \quad \text{... (6)}$$

The calculated values (**Table-4**) suggest a covalent bonding[43,46,72]. The in-plane and out of- plane π-bonding coefficients B_1^2 and B^2 respectively, are dependent upon the values of ΔE_{xy} and ΔE_{xz} in the following equations[65].

$$\alpha^2 \beta^2 = (g_{\perp} - 2.002)\, \Delta E_{xy}/2\lambda_o \quad \text{… (7)}$$

$$\alpha^2 \beta_1^2 = (g_{\|} - 2.002)\, \Delta E_{xz}/8\lambda_o \quad \text{… (8)}$$

In this work, the complex **(3)** shows β^2 and β_1^2 values 0.79 and 0.71 indicating a moderate degree of covalency in the in-plane and out of- plane[75]. It is possible to calculate approximate orbital populations for s, p or d orbitals[76] by

$$A_{\|} = A_{iso} - 2\beta\, [1 \pm (7/4)\, \Delta g_{\|}] \quad \text{… (9)}$$

$$a^2_{p,d} = 2\beta / 2\beta^\circ \quad \text{…(10)}$$

Where A° and 2B° are the calculated dipolar coupling for unit occupancy of s and d orbitals respectively. The calculated orbital publication for the copper (II) complex **(3),** (**Table-4**), indicate a $d_{(x2-y2)}$ ground state[40]. Manganese (II) complex **(5),** cobalt (II) complex **(6)**, chromium (III) complex **(12)** and iron (III) complex **(13)** show isotropic type with g_{iso}= 2.006, 2.03, 2.1 and 2.13 respectively indicating octahedral structure around the metal ion[46,66].

Thermal Analyses [DTA and TGA]: Since the IR spectra indicate the presence of water molecules, Thermal analyses (DTA and TGA) were carried out to a certain nature. The thermal curves in the temperature 27 - 800°C range for complexes **(2), (4), (9)** and **(13)** are thermally stable up to 35°C. For Cu (II) complex **(2)**, breaking of hydrogen bond is characterized by endothermic peak at the temperature 40°C. Dehydration is characterized by endothermic peaks at the temperature 75°C, with 5.4% weight loss (Calc. 4.88%) corresponding to the loss of two hydrated water molecule[77-79].

The decomposition step for complex **(2)** occurred at 137°C with 10.77 % weight loss (Calc. 10.27%), which could be due to the elimination of four coordinated H_2O. Another thermal decomposition at 291 with 19.11 % weight loss (Calc. 18.75 %), which could be due to the loss of two coordinated acetate group. Endothermic peak observed at 416°C may be due to melting point.

Finally, the complex shows exothermic peaks in the 456-500°C range, corresponding to oxidative thermal decomposition which proceeds slowly with 17.2% weight loss (Calc. 16.73%) which could be due to the loss of two CuO [78]. Ni (II) complex **(4)** shows endothermic peak at 59°C, with 4.46% weight loss (Calc. 4.9%), due to two hydrated water molecule, however, the endothermic peak observed at 182°C with 10.7% weight loss (Calc. 10.4%), assigned to four coordinated water molecules, another peak is observed

at 331°C with 19.6% weight loss (Calc. 19.03%), assigned to two coordinated acetate group, the endothermic peak observed at 386°C may be assigned to the melting point. Oxidative thermal decomposition occurs in the 450 - 575°C range with exothermic peaks, leaving 2NiO 28.9% weight loss (Calc. 29.48%)[80,81]. Zn(II) complex **(9)** shows endothermic peak at 51°C with 13.33% weight loss (Calc. 12.88%) which indicate loss of two hydrated water molecule, however, endothermic peak observed at 173 with 7.5% weight loss (Calc. 7.39%) due to coordinated water molecules, another endothermic peak observed at 444°C may be assigned to the melting point.

Oxidative thermal decomposition occurs in the 450-590°C range with exothermic peaks, leaving ZnO. Finally, Fe (III) complex **(13)** shows endothermic peak at 59°C with 11.9% weight loss (Calc. 11.2%) due to the loss of four hydrated water molecule, another endothermic peak is appeared at 135°C with 18.5% weight loss (Calc. 19.1%) is assigned to the loss of three coordinated chlorine molecules. The endothermic peak appears at 351°C may be assigned to the melting point. Oxidative thermal decomposition occurs in the 450-674°C range with exothermic peaks, leaving Fe_2O_3 with 35.2% weight loss (Calc. 34.756%)[81].

BIOLOGICAL STUDIES

Concentration (µg)	**Surviving factor of metal complexes (2), (4), (7), (8) and (13)**					
	standard	complex(2)	complex(4)	complex(7)	complex(8)	complex(13)
concentrartion (50)	26.21	31.26	53.24	64.82	55.21	56.24
concentrartion (25)	18.89	40.88	67.56	79.54	68.96	65.92
concentrartion (12.5)	21.1	56.16	79.08	84.15	79.38	73.86
concentrartion (6.25)	31.8	72.64	88.44	89.66	85.13	86.22
concentrartion (3.125)	73.1	96.28	97.52	97.12	96.38	98.14
concentrartion (1.56)	88.5	100	100	100	100	100

Antitumor activity: The antitumor effect of the ligand (**1**) and its metal complexes **(2), (4), (7), (8)** and **(13)** in DMSO were evaluated against heptocellular carcinoma (HePG- 2 cell line), **Figure 3**.

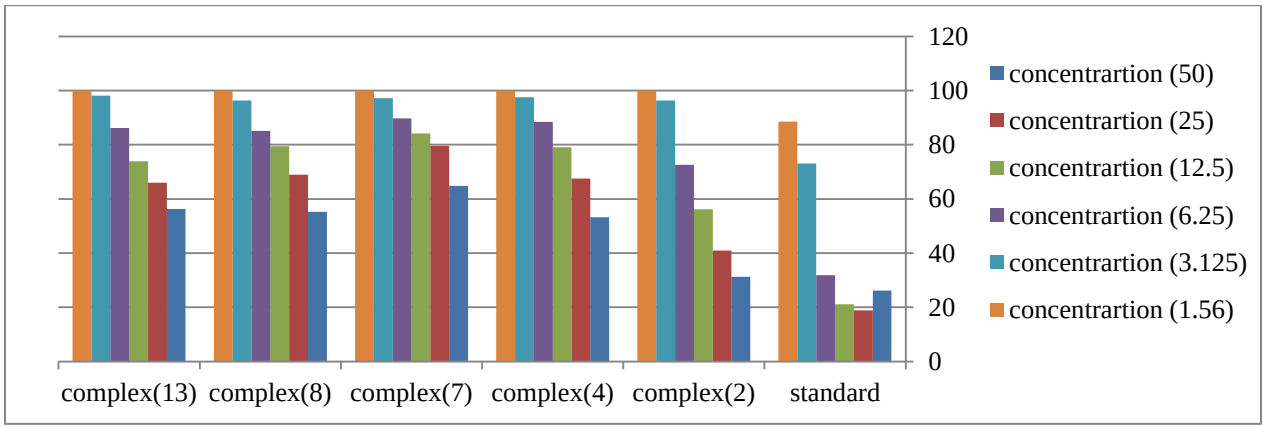

Figure 3: Cytotoxicity of standard drug and metal complexes **(2), (4), (7), (8) and (13)** against HePG- 2 cell line.

These were tested by comparing them with the standard drug (Sorafenib). The solvent DMSO showed no effect on cell growth as it was reported previously [82] .The ligand **(1)**, showed a weak inhibition effect at ranges of concentrations used, however, the complexes showed moderate effect against HePG- 2 cell line as shown in **Table-7**. Also. This could be explained as complex could bind to DNA where it seemed that, change the anion and the nature of the metal ion in complexes may have effect on the biological behavior, by altering the binding ability of DNA[82-86].

Moreover, Gaetke and Chow had reported that, metal has been suggested to facilitate oxidated tissue injury through a free-radical mediated pathway analogous to the Fenton reaction[87]. Also, it was shown that, the resulting Cu (I) complexes are also able to form GSSG via the following reactions:

$$[\text{Cu (I) (ligand)}] + \text{GSH} \rightarrow [\text{Cu (I) (GS)}] + \text{ligand} + \text{H}^+ \quad \ldots (1)$$

$$[\text{Cu (I) (GS)}] + \text{GS}^+ \rightarrow [\text{Cu (II)} + \text{GSSG} \quad \ldots (2)$$

These reactions lead to depletion of intracellular GSH pools, which has been frequently observed in cells after treatment with diverse Cu compounds[88-90]. In the presence of H_2O_2, the DNA-bound Cu(II) complex is oxidized to form presumably Cu(II) (oxo/ hydroxo) species[91,92], thus, the reaction of Cu(II) complex with nucleic acid is via Cu-oxo/ hydroxo intermediate[93]. Cu (II) complexes are well known for their redox activity, which seems to be responsible for biological activities[89,94,95].

The redox cycling of Cu complexes is based on the reduction of Cu (II) to Cu (I) by intracellular thiols such as GSH (glutathione, nonenzymatic antioxidant under oxygen-contaning conditions [90, 96, 97]. Schematically, the underlying reaction pathway for [Cu (II) (ligand)] complexes is given in **equations (1, 2)**. Briefly, Cu (II) complexes rapidally form adducts with GSH[96,98], leading to Cu (I) complexes and GS^+. In the presence of oxygen, this Cu (I) complex is able to generate a superoxide anion, which can induce ROS via a fenton- like reaction:

$$[\text{Cu (II) (ligand)}] + \text{GSH} \rightarrow [\text{(GS) Cu (II) (ligand)}] + \text{H}^+ \quad \ldots (3)$$

$$[\text{(GS) Cu (II) (ligand)}] \rightarrow [\text{GS}^+ + [\text{Cu (I) (ligand)}] \quad \ldots (4)$$

$$[\text{Cu (I) (ligand)}] + \text{O}_2 \rightarrow \text{O}_2^{\cdot} + [\text{Cu (II) (ligand)}] \quad \ldots (5)$$

By applying the ESR-trapping technique, evidence for metal-mediated hydroxyl radical formation invivo has been obtained[72]. Radicals are produced through a Fenton-type reaction as follows[87]:

$$\text{LM (II)} + \text{H}_2\text{O}_2 \rightarrow \text{LM (I)} + {}^{\cdot}\text{OOH} + \text{H}^+$$

$$\text{LM (I)} + \text{H}_2\text{O}_2 \rightarrow \text{LM (II)} + {}^{\cdot}\text{OH} + \text{OH}^-$$

Where L is the ligand

Also, metal could act as a double-edged, sword by inducing DNA damage and also by inhibiting their repair[98]. The OH radicals react with DNA sugars and bases and the most significant and well-characterized of the OH reactions is hydrogen atom abstraction from the C_4 atom to yield sugar radicals with subsequent β-elimination. **Scheme 2**, by this mechanism strand breakage occurs as well as the

release of the free bases. Another form of attack on the DNA bases is by solvated electrons, probably via a similar reaction to those discussed below for the direct effects of radiation on DNA[74].

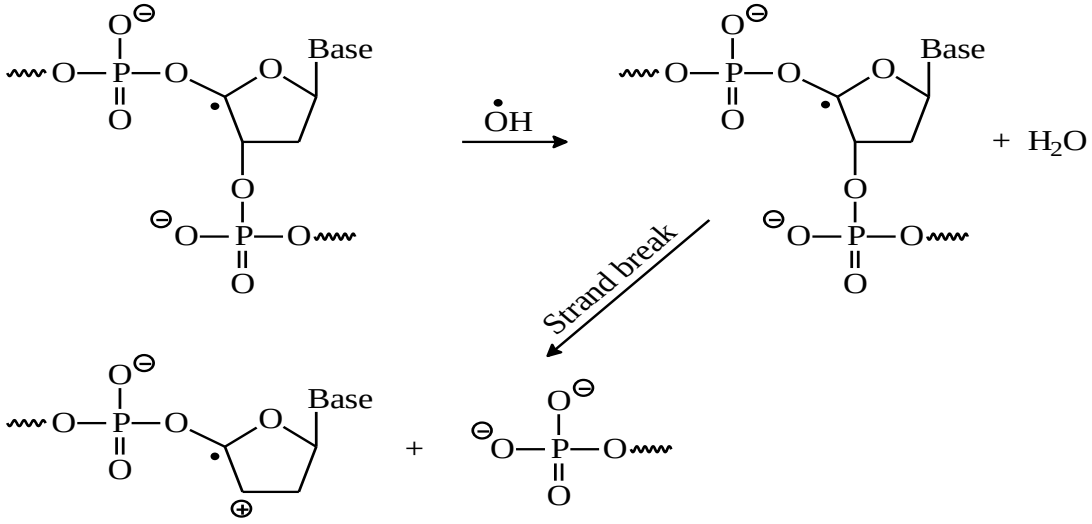

Scheme-2

The relation between the concentration of the complexes in DMSO and their anti-proliferative activity are shown in **Table-7** and **Figures (2)-(13)**. Although, complexes were octahedral structures and had the same anions, the variable activity of the complexes might be due to their oxidation–reduction potentials. Intercalative binding of metal complex of guanidine to DNA resulting from the insertion of metal complex between the base pairs of the DNA douple helix. The binding mode of the guanidine group depends on a great extent not only on the nature of the metal ion but on the presence of the neighboring donor group in the same chelate rings upon coordination to metal ion[97,98]. Complexes 4-(di 1, 3(2-hydroxybenzylidene) guanidino)-benzoic acid ligand showed inhibitory activity against hepatocellular carcinoma (HepG-2 cell line).

Table-7:

The concentration	**Order of antiproliferative effect of the studied complexes**
At concentration 50µg/ml	standard > Cu(II) complex (2) > Ni(II) complex (4)> Hg(II) complex (8) > Fe(III) complex (13) > UO_2(II) complex (7)
At concentration 25 µg/ml	standard > Cu(II) complex (2) > Fe(III) complex (13) >Ni(II) complex (4)> Hg(II) complex (8) > UO_2(II) complex (7)
At concentration 12.5 µg/ml	standard > Cu(II) complex (2) > Fe(III) complex (13) >Ni(II) complex (4)> Hg(II) complex (8) > UO_2(II) complex (7)
At concentration 6.25 µg/ml	standard > Cu(II) complex (2) > Hg(II) complex (8) >Fe(III) complex (13) >Ni(II) complex (4)> UO_2(II) complex (7)
At concentration 3.125 µg/ml	standard > Cu(II) complex (2) > Hg(II) complex (8) > UO_2(II) complex (7) >Ni(II) complex (4)> Fe(III) complex (13)
At concentration 1.56 µg/ml	standard > Cu(II) complex (2) = Ni(II) complex (4) = Hg(II) complex (8) = Fe(III) complex (13) = UO_2(II) complex (7)

Antifungal screening: The ligand **(1)** and its metal complexes have been screened for their antifungal activities **Figure (4)**. The results show that, complexes **(2), (3), (4), (5), (6), (7), (9), (12), (15)** and **(16)** have no effect on Asperigellus Niger, however, complexes (**8**), **(10) and (11)** exhibit highest antifungal activity compared with other complexes. The order of the complexes is, complex **(10)** > complex **(11)** > complex **(8)**. This enhancement in the activity can be explained on the basis of chelation theory[99,100]. Chelation reduces the polarity of the metal ion considerably, mainly because of the partial sharing of its positive charge with donor groups and possible π-electron delocalization on the whole chelation ring. The lipid and polysaccharides are some important constituents of cell wall and membranes, which are preferred for metal ion interaction. In addition to this, the cell wall also contains many amino phosphates, carbonyl and cystenyl ligands, which maintain the integrity of the membrane by acting as diffusion and also provide suitable sites for bonding.

Hg (II) complex (**8**) Tl (I) complex (**11**)

Cd (II) complex (**10**) Cu (II) Complex (2) negative

Figure (4): Inhibition zone of Hg (II) complex (**8**), Cd (II) complex (**10**) and Tl (I) complex (**11**).

Chelation can reduce not only the polarity of the metal ion, but also increases the lipophilic character of the chelate and the interaction between metal ion and the lipid is favored. This may lead to the breakdown of the permeability barrier of the cell resulting in interference with the normal cell processes. Some important factors such as the nature of the metal ion, nature of the ligand, coordinating sites and geometry of the complex, concentration, hydrophilicity, lipophilicity and presence of co-ligands have considerable influence on antifungal activity[99,100]. Certanly, steric and pharmacokinetic factors also play a decisive role in deciding the potency of an antifungal agent. Apart from this, the mode of the action of these compounds may also invoke hydrogen bond through the >C=N-N-CH- group with the active centers and thus interfere with normal cell process. The presence of lipophilic and polar substituents is expected to enhance antifungal activity. The antifungal activity of the guanidine ligands and their metal complexes were screened using the disk diffusion. The variation in the activity of different complexes against different microorganisms depends either on the impermeability of the cells of the microbes or differences in ribosomes in microbial cells.

Antibacterial screening: In vitro biological screening tests of the ligand **(1)** and its complexes were carried out as antibacterial activity, **Figure (5)**. The antibacterial activity was tested against two bacterial strains: gram positive bacteria (Streptococcus and Enterococcus), the results compared with standard drug (Ampicillin), and gram negative bacteria (Klebsiella pneumoniae and salmonella) strains, the results compared with standard drug (Gentamycin). The data indicated that, complexes were active against bacteria. Complexes of Cu(II) complex (3), Ni (II) complex (4) and Cd(II) complex (10) with Schiff bases show antibacterial activities against gram positive bacteria (Streptococcus and Enterococcus) and gram negative bacteria (Klebsiella pneumoniae and salmonella).

Bacteria	Inhibition mean zone of metal complexes (**3**), (**4**) and **(10**) against gram positive and negative bacteria			
	Standard	complex(3)	complex(4)	complex(10)
Streptococcus	26	13.2	16.9	19.8
Enterococcus	20	15.3	19.3	21.4
Klebsiella pneumoniae	22	14.6	17.3	20.6
Salmonella	28	15.3	19.3	21.3

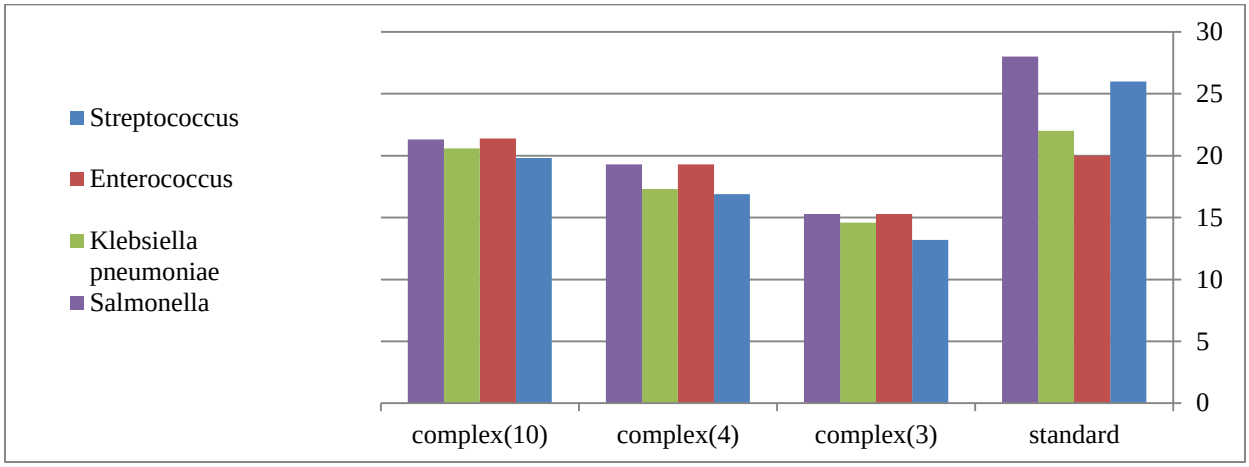

Figure 5: Inhibition mean zone of metal complexes (**3**), (**4**) and (**10**) against gram positive and gram negative bacteria.

The results showed that, the metal complexes have a greater effect than ligand against bacteria[101]. Cadmium (II) complexes showed wide range of bactericidal activities against gram negative bacteria and gram positive bacteria. Whereas Cu (II), and Ni (II) are moderately active against both gram negative bacteria and gram positive bacteria. The agar well-diffusion method was tested and each experimental was performed in triplicate. The zone of inhibition value represents the mean value of three readings. The antibacterial studies demonstrated that, Cu (II) complex (**3**), Ni (II) complex (**4**) and Cd (II) complex (**10**) have activity toward tested bacteria whereas the ligand and Cr (III) complex (**12**) show no activity. Besides these, the inhibition of bacteria growth increases with decreases the concentration of these complexes using 5 mg/ml concentration of tested samples as shown in **Table-8**. The relation between the inhibition mean zone of Cu (II) complex (**3**),Ni (II) complex (**4**) and Cd (II) complex (**10**) against Streptococcus, Enterococcus, Klebsiella pneumoniae and salmonella are showed in **Figure 5** (Please specify the figure 8)

Table-8:

The Bacteria	**Order of antibacterial (+ve) effect of the studied complexes**
Streptococcus	standard > Cd(II) complex (10) > Ni(II) complex (4) > Cu(II) complex (3)
Enterococcus	Cd(II) complex (10)> standard > Ni(II) complex (4) >Cu(II) complex (3)

Table-8B:

The Bacteria	**Order of antibacterial (-ve) effect of the studied complexes**
Klebsiella pneumoniae	standard > Cd(II) complex (10) > Ni(II) complex (4) > Cu(II) complex (3)
Salmonella	standard > Cd(II) complex (10) > Ni(II) complex (4) > Cu(II) complex (3)

CONCLUSION

Cr (III), Mn (II), Fe (III), Co (II), Ni (II), Cu (II), Zn (II), Cd (II), Sr (II), Hg (II), Tl (I), UO_2 (II) and ZrO (II) complexes of (4-(di 1,3(2-hydroxybenzylidene) guanidino) benzoic acid ligand have been prepared and spectrally characterized. The IR data show that, the ligand behaves as dibasic hexadentate, monobasic tetradentate, dibasic tetradentate. Molar conductances in DMF indicate that, the complexes are non-

electrolyte. The ESR spectra of solid Cu (II) complex **(3)** at room temperature show axial type symmetry with $g_{//} > g_{\perp} > 2.0023$, indicating a $d_{(x2-y2)}$ ground state with significant covalent bond character in square planar geometry. However, Cu (II) complex **(2)** shows broad signals in the low and high field regions indicating spin – spin interactions takeplace between Cu (II) ions through deprotonated hydroxyl group. Complexes Mn (II) complex **(5)** and Co (II) complex **(6)**, Cr (III) complex **(12)** and Fe (III) complex **(13)** show isotropic type with g_{iso}= 2.006, 2.03, 2.1 and 2.13 respectively indicating octahedral structure around the metal ion. Cu (II) complex **(2)**, Ni (II) complex **(4)**, UO_2 (II) complex **(7)**, Hg (II) complex **(8)** and Fe (III) complex **(13)** showed inhibitory effect on liver carcinoma (HePG- 2 cell line) in comparing with the standard drug.

ACKNOWLEDGMENTS

We thank Dr Abdou Saad El-Tabl (Chemistry Department, Faculty of Science, Menoufia University, Shebin El- Kom, Egypt), Dr Moshira Mohamed Abd El-wahed (Pathology Department, Faculty of Medicine, Menoufia University, Shebin El- Kom, Egypt) for their scientific input to our report.

REFERENCES

1. K. Ertell, recycled paper, A Review of Toxicity and Use and Handling Considerations for Guanidine, Guanidine Hydrochloride, and Urea Prepared for the U.S. Department of Energy, 2006, 3-9.
2. J. Kobayashi and M. Ishibashi, Marine natural products and marine chemical ecology, in Comprehensive Natural Products Chemistry (eds D. Barton and K. Nakanishi), 1999, **8**, 415–649.
3. G. Murtaza, M. K. Rauf, A. Badshah, M. Ebihara, M. Said, M. Gielen, D. de Vos, E. Dilshad, B. Mirza, *Eur. J. Med. Chem*., 2012, **48**, 26.
4. L. Feng, F. Wu, J. Li, Y. Jiang, X. Duan, *Postharvest Biol. Technol*., 2011, **61**, 160.
5. T. Satoh, M. Muramatu, Y. Ooi, H. Miyataka, T. Nakajima, M. Umeyama, *Chem. Pharm. Bull*., 1985, **33**, 647.
6. Y. Miyamoto, H. Hirose, H. Matsuda, S. Nakano, M. Ohtani, M. Kaneko, K. Sishigaki, F. Nomura, H. Kitamura, Y. Kawashima, *Trans. Am. Soc. Artif. Int. Organs*., 1985, **31,** 508.
7. K. Omura, Y. Kiyohara, F. Komada, S. Iwakawa, M. Hiral, T. Fuwa, *Pharm. Res*., 1990, **7,** 1289.
8. I. Muramatsu, M. Oshita, K. Yamanaka, *J. Pharmacol*., 1983, **227**, 194-198.
9. S. Umezawa, Y. Takahashi, T. Usui, T. Tsuchiya, *J. Antibiot*., 1974, **27**.
10. S. Marriner, *Vet. Rec*., 1986, **118,** 181.
11. B. L. Freedlander, F. A. French, *Cancer Res*., 1958, **18**, 360.
12. G. J. Durant, W. A. Duncan, C. R. Ganellin, M. E. Parsons, R. C. Blakemore, *Nature*., 1978, **276**, 403.
13. K. Rudolf, W. Eberlein, W. Engel, H. A. Wieland, K. D. Willim, Entzeroth, M. Wienen, W. Beck-A. G. Sickinger, H. N. Doods, *Eur. J. Pharmacol*., 1994, **271**, R11-R13.
14. W. Sang, Z. Tang, M. Y. Hea, Y. P. Huab, Q. Xu, *Int. J. of Biological Macromolecules*, 2015, **75**, 489.

15. B. Billach, D. E. Heck, D. M. Porterfield, R. P. Salchow, P. J. S. Smith, C. R. Gardnem, D. L. Laskin, J. D. Laskin, *Biochem. Pharmacol*., 2011, **61,** 1581.
16. M. A. Mansour, A. M. Mustafa, M. N. Nagi, M. M. Khattab, O. A. Al-Shabanah, *Comp. Biochem. Physiol*., 2002, **132,** 123.
17. J. H. Van den Berg, J. H. Beijnen, A. J. M. Balm, J. H. M. Schnellens, *Cancer Treat. Rev*., 2006, **32,** 390.
18. A. S. Abdel-Naby, R. F. Al-Ghamdi, A. A. Al-Ghamdi, *Journal of vinyl &additive technology*, 2010, **1002**, 15.
19. K. F. Khaled, *Int. J. Electrochem. Sci*., 2008, **3,** 474.
20. H. M. Hua, J. Peng, D. C. Dunbar, R. F. Schinazi, A. G. C. Andrews, C. Cuevas, L. F. Garcia-Fernandez, M. Kelly, M. T. Hamann, *Tetrahedron*, 2007, **63**, 11179.
21. M. Zarraga, A. M. Zarraga, B. Rodriguez, C. Perez, C. Paz, P. Paz, C. Sanhueza, *Tetrahedron Lett*., 2008, **49,** 4775S.
22. A. I. Vogel, A text Book of Quantitative Inorganic Analysis (Longman Suffolk), 1961.
23. J. Lewis, R. G. Wilkins, *Modern Coordination Chemistry. Interscience*. New York, **1960**, 403.
24. P. Skehan, R. Storeng *et al*., *J. Natl. Cancer Inst*., 1990, **82**, 1107.
25. A. S. El-Tabl, S. A. El-Enein, *J. Coord. Chem*., 2004, **57**, 281.
26. M. F. R. Fouda, M. M. ABD- El- Zaher, M. M. Shakdofa, F. A. El- Sayed, M. I. Ayad, A. S. El-Tabl, *J. Coord. Chem*., 2008, **61**, 1983.
27. A. S. El-Tabl, M. Abd-Elwahed, M. H. Mohammed, *Chemical Speciation & Bioavailability*, 2013, **25,** 143-145.
28. F. El- Mariah, *J. Chem. Resa*., 2009, 588.
29. S. Mayadevi, P. G. Prasad, K. K. M. Yusuff, *Synth and Rea in Inorg and Met.Org. Chem*., 2003, **33**, 481.
30. A. S. El-Tabl, R. M. El-Bahnasawy, M. M. Shakdofa, E. A. El-Deen Abdalah, *J. Chem., Reas*., 2010**,** 88.
31. R. S. Baligar, V. K. Revankar, *J. Serb. Chem. Soc*. 2006, **71**, 1301.
32. W. J. Geary, *Coord. Chem. Rev*., 1971, **7,** 81.
33. A. S. El-Tabl, F. A. El-Sayed, A. N. Al-Hakimi, *Trans. Met. Chem*., 2004, **57**, 265.
34. A. S. El-Tabl, *Trans. Met. Chem*., 1997, **22,** 400.
35. E. Tas, M. Aslanoglu, A. Kilic, Z. Tara, *Trans. Met. Chem*., 2005, **30**, 758.
36. S. Chandra, U. Kumar, *Spectrochim. Acta part*, 2005, **61**, 219.
37. S. K. Nakamoto, Infrared and Raman spectra of Inorganic and Coordination Compounds, 3 rded, John Wiley & Sons, New York, 1977, 244-247.
38. N. S. Youssef, E. El-Zahery, A. M. A. El-Seidy, *Phosphorous, sulfur and silicon*, 2010, **185,** 785.
39. A. S. El-Tabl, F. A. El-Saied, A. N. Al-Hakimi, *Trans. Met. Chem*., 2007, **32**, 689.
40. A. S. El-Tabl, K. El-Baradie, R. M. Issa, *J. Coord. Chem*., 2003, **56**, 1113.
41. A. S. El-Tabl, *J. Res*. 2002, 529.
42. A. S. El-Tabl, R. M. Issa, *J. Coord. Chem*., 2004, **57**, 509.
43. A. S. El-Tabl, F. A. El-Saied, A. N. Al-Hakimi, *J. Coord. Chem*., 2008, **61,** 2380.
44. H. A. Kuska, M. T. Rogers, Coordination chemistry, A. E. Martell, Ed: Van Nostrad Reihold Co: New York, 1971.
45. S. D. Roenson, M. F. Uttly, *J. Chem. Soc. Dalton Trans*., 1973, 1912.

46. R. M. El-Bahnasawy, A. S. El-Tabl, E. El-shereafy, T. I. Kashar, Y. M. Issa, *Polish J. Chem*., 1999, **73,** 1925.
47. A. N. Al-Hakimi, M. M. E. Shakdofa, A. M. El- Seidy, A. S. El-Tabl, *J. Korean Chem. Soc*., 2001, **55,** 418.
48. R. A. Lai, A. Kumar, *Ind. J. Chem*., 1999, **38A**, 839.
49. N. Raman, Y. Pitchaikani, A. Kulandaisamy, *Proc. Indian Acat. Sci (Chem. Sci)*., 2001, **133**, 183.
50. K. B. Gudasi, S. A. Patel, R. S. Vadvavi, R. V. Shenoy, M. Nethaji, *Transition Met. Chem*., 2006, **31**, 586.
51. J. K. Nag, S. Pal, C. Sinha, *Transition Met. Chem*., 2005, **30**, 523.
52. B. M. Urukan, K. Mohanan, *Transition Met. Chem*., 2006, **31**, 441.
53. K. B. Gudasi, S. A. Patil, R. S. Rashmi, V. Shenoy, M. Nethaji, *Transition Met. Chem*., 2006, **31,** 580.
54. E. W. Ainscough, A. M. Brodie, A. J. Dobbs, J. D. Ranford, J. M. Waters, *Inorg. Chem. Acta*, 1998, **267**, 27.
55. S. A. Sallam, A. S. Orabi, B. A. El-Shetary, A. Lentz, *Trans. Met. Chem*., 2002, **27,** 447.
56. V. Ravinder, S. J. Swamy, S. S. Srihari, P. Longaiah, *Polyhedron*, 1985, **4**, 1511.
57. R. Atkin, G. Brewer, E. Kokot, G. M. Mochier, E. Sinn, *Inorg. Chem*., 1985, **24,** 127.
58. N. V. Takkar, S. Z. Bootwala, *Indian J. Chem*., 1995, **34A,** 370.
59. G. C. Chinvmia, D. J. Phillips, A. D. Rae, *Inorg. Chim. Acta*, 1995, **238**, 197.
60. C. H. Krishna, C. M. Mahapatra, K. C. Dush, *J. Inorg. Nucl. Chem*., 1997, **39**, 1253.
61. R. K. Parihari, R. K. Patel, R. N. Patel, *J. Ind. Chem. Soc*., 2000, **77,** 339.
62. F. Sabin, A. Vogler, *Monta. Chem*., 1992, **123,** 705.
63. N. K. Singh, S. B. Singh, *Transition Met. Chem*., 2001, **26**, 487.
64. G. M. Abu El-Reash, K. M. Ibrahim, M. M. Bekheit, *Trans. Met. Chem*. 1990, **15**, 148.
65. B. P. Lever, Inorganic Electronic Spectroscopy, Elsevier pub. Company, New York. 1968, 275.
66. A. S. El-Tabl, *Bull. Korean Chem. Soc*., 2004, **25,** 1.
67. A. S. El-Tabl, M. M. E. Shakdofa, A. M. El-Seid, *J. Korean Chem. Soc*. 2011, **55** 603.
68. H. A. El-Boraey, A. S. El-Tabl, *Polish J. Chem*., 2003, **77,** 1759.
69. A. S. El-Tabl, *Trans. Met. Chem*., 1998, **23,** 63.
70. M. Procter, B. J. Hathaway, P. N. Nicholls, *J. Chem. Soc. (A)*, 1969, 1678.
71. D. E. Nickless, M. J. Power, F. L. Urbach, *Inorganic Chem*., 1983, **22**, 3210.
72. R. K. Ray, *Inorg. Chim, Acta*, 19990, **174**, 257.
73. A. S. El-Tabl, *J. Chem. Resea*. 2004, 19.
74. D. Kivelson, R. Neiman, *J. Chem. Phys*. 1961, **35,** 149.
75. D. W. Smith, *J. Chem. Soc. A*, 1970, 3108.
76. M. M. Bhadbhade, D. Srinivas, *Inorg. Chem*., 1993, **32,** 2458.
77. M. C. R. Symons, Chemical and Biological Aspects of Electron Spin Resonance, Van Nostrand Reinhold, Wokingham. 1979.
78. C. Natarajian, P. Shanthi, P. Athappan, R. Murugesan, *Trans. Met. Chem*., 1992, **17,** 39.
79. J. A. Bertrand, T. D. Black, P. G. Eller, F. T. Helm, R. Mahmood, *Inorg. Chem*., 1976, **15,** 2965.
80. A. S. El-Tabl, S. M. Imam, *Trans. Met. Chem*., 1997**,** 21.
81. M. Gaber, M. M. Ayad, *Thermochim. Acta*, 1991, **176,** 21.
82. A. S. El-Tabl, M. M. Abou-Sekkina, *Polish J. Chem*., 1999, **73**, 1937.

83. N. A. Illan-Cabeza, A. R. Garcia–Garcia, M. N. Moreno–carretero, J. M. Martinez–Martos, M. I. Ramirez–exposito, *J. Inorg. Biochem*., 2005, **99,** 1637-1645.
84. H. Hall, C. C. Lee, G. Ibrahim, M. A. Khan, G. M. Bouet, *Appl. Organomet. Chem*., 1997, **11,** 565-575.
85. G. Feng, J. C. Mareque-Rivas, R. T. Rosales, N. H. Williams, *J. Am. Chem. Soc*., 2005, **127**, 13470-13471.
86. J. C. Mareque, R. Prabaharan, S. Parsons, *Dalton Trans*., 2004, **21**, 1648-1655.
87. Bauer-Siebenlist, F. Meyer, E. Farkas, D. Vidovic, S. Dechert, *J. Chem. Eur*., 2005, **11**, 4349-4360.
88. L. M. Gaetke, C. K. Chow, *Toxicology*, 2003, **189**, 147-163.
89. M. F. Khan, Y. Ohno, A. Takanaka, *Arch Toxicol*., 1992, **66**, 587–591.
90. M. McCann, M. Geraghty, M. Devereux, D. O'Shea. J. Mason, L. O'Sullivan, *Met Based Drugs*, 2000, **7**, 185-193.
91. J. Narasimhan, W. E. Antholine, C. R. Chitambar, D. H. Petering, *Arch Biochem Biophys*., 1991, **289**, 393-398.
92. L. E. Marshall, D. R. Graham, K. A. Reich, D. S. Sigman, *Biochemistry*, 1981, **20**, 244–250.
93. D. S. Sigman, A. Mazumder, D. M. Perrin, *Chem Rev*., 1993, **93**, 2295–2316.
94. R. W. Byrnes, W. E. Antholine, D. H. Petering, *Free Radic Biol Med*., 1992, **13**, 469–478.
95. O. Zelenko, J. Gallagher, Y. Xu, D. S. Sigman, *Inorg Chem*., 1998, **37**, 2198-2204.
96. L. A. Saryan, K. Mailer, C. Krishnamurti, W. Antholine, D. H. Petering, *Biochem Pharmacol*., 1981, **30**, 1595-1604.
97. A. Rouzer, *Chemical Research in Toxicology*, 2010, **23**, 1517-1518.
98. M. Duda, A. Karaczyn, H. Kozlowski, I. O. Fritsky, T. Glowiak, E. V. Prisyazhnaya, T. Y. Sliva, J. S. Kozlowskac, *J. Chem. Soc. Dalton Trans*., 1997, 3853.
99. J. Custot, J. L. Boucher, S. Vadon, C. Guedes, S. Dijols, M. elaforge, Mansuy, *J. Biol. Inorg. Chem*., 1995, **1**, 73.
100. T. J. Franklin and G. A. Snow, Biochemistry of Antimicrobial Action, 2nd edn., Chapman and Hall, London, 1971.
101. C. H. Collins and P. M. Lyn, Microbial Methods, University, Park Press, Baltimore, 1970.
102. E. Ispir, S. Toroglu, Z. A. Kayraldi, *Transition Met Chem*., 2008, **33**, 953.

***Corresponding author: Abdou Saad El-Tabl;**

Department of Chemistry, Faculty of Science, El-Menoufia University, Shebin El-Kom, Egyp